Synthesis, Structure, and Dielectric Properties of $(Bi_{1/2}Ag_{1/2})TiO_3$

J.-H. Park,[†] P. M. Woodward,[⊥,‡] J. B. Parise,*[,†,§] R. J. Reeder,[§] I. Lubomirsky,[∥] and O. Stafsudd[∥]

Center for High-Pressure Research, Department of Chemistry and Department of Geosciences, State University of New York, Stony Brook, New York 11790-2100, Physics Department, Brookhaven National Laboratory, Upton, New York 11973, and Department of Electrical Engineering, University of California at Los Angeles, Los Angeles, California 90024

Received September 18, 1998. Revised Manuscript Received November 10, 1998

The compound $Bi_{1/2}Ag_{1/2}TiO_3$ has been synthesized, for the first time, at 14−14.5 GPa and 1000 °C using the uniaxial split sphere anvil type press (USSA-2000). The structure of the quenched powder sample was refined from synchrotron X-ray diffraction data using the Rietveld method. At room temperature, $Bi_{1/2}Ag_{1/2}TiO_3$ exhibits an orthorhombic distortion of the cubic perovskite structure and was assigned to a space group of *Ibam* and lattice parameters of $a = 5.48970(4)$ Å, $b = 5.51954(5)$ Å, and $c = 7.77585(7)$ Å. The refinements are consistent with a random distribution of Bi^{3+} and Ag^{+} on the A-sites. Diffraction results at various temperatures show two phase transitions as the temperature is increased. At 573 K, tetragonal symmetry is observed and was assigned to a space group of $I4/mcm$ with lattice parameters of $a = 5.51664(8)$ Å and $c = 7.8134(2)$ Å, while at 673 K, the cubic perovskite structure, with space group $Pm\bar{3}m$ and $a = 3.90607(8)$ Å, was determined. Plane capacitor dielectric contact measurements at 100 kHz gave a dielectric constant of 354 at ambient temperature for the sample. The dielectric constant increases with temperature and reaches a local maximum of 834 at 578 K. After heating the sample to 778 K and cooling back to room-temperature, both dielectric and diffraction measurements provide evidence for a small but irreversible change in the stoichiometry.

Introduction

Materials belonging to the perovskite structure class have attracted widespread scientific and technological interest over the past 40 years. This interest can be largely attributed to the discovery of ferroelectricity in compounds such as $BaTiO_3$, $PbTiO_3$, and $Pb(Mg_{1/3}Nb_{2/3})O_3$.[1] In these materials both A-site (i.e. Pb^{2+}) and B-site cations (i.e. Ti^{4+}) can play an important role in the development of spontaneous polarization. Among those perovskite materials which show ferroelectric and/or piezoelectric behavior, a common feature is the presence of a highly polarizable cation, such as Pb^{2+}, on the A-site. The high polarizability of Pb^{2+} is in many cases greatly enhanced by the presence of a stereochemically active electron lone pair. The Bi^{3+} ion, which is isoelectronic with Pb^{2+}, is also known to commonly show a lone pair effect. This has led some researchers to look toward perovskites containing Bi^{3+} as alternatives to the lead-based ferroelectric and piezoelectric materials. However, there are relatively few perovskites which contain Bi^{3+} on the A-site;[2−4] among these, $(Bi_{1/2}Na_{1/2})TiO_3$ (BNT) has been the most extensively probed for its interesting dielectric properties.[5]

At room temperature the structure of BNT is rhombohedral, with space group $R3c$.[6] A transformation to tetragonal symmetry occurs in the temperature range 200−340 °C, followed by a transition to cubic symmetry above 540 °C.[7] Structural details of the high-temperature phases are still rather limited. The diffuse nature of the rhombohedral−tetragonal phase transition has prevented any detailed structural study of the tetragonal phase. Park et al. report weak superstructure reflections in the high-temperature cubic phase, which can be indexed using a face-centered cubic cell with cell edge twice that of a simple perovskite.[8] They take this observation as proof of partial Na^{+}/Bi^{3+} ordering, in agreement with suggestions made in previous studies.[9,10] However, since no evidence is provided to estab-

[†] Department of Chemistry, State University of New York.
[⊥] Current address: Department of Chemistry, The Ohio State University, Newman and Wolfrom Laboratory, 100 West 18th Avenue, Columbus, OH 43210-1185.
[‡] Brookhaven National Laboratory.
[§] Department of Geosciences, State University of New York.
[∥] University of California at Los Angeles.

(1) Galasso, F. S. *Structure, Properties and Preparation of Perovskite-type Compounds Chapter 5*; Pergamon Press: Oxford, 1969.
(2) Michel, C.; Moreau, J.-M.; Achenbach, G.; Gerson, G.; James, W. *J. Solid State Commun.* **1969**, *7*, 701.
(3) Iwahashi, K.; Iida, S. *J. Phys. Soc. Jpn.* **1965**, *20*, 1526.
(4) Ivanova, V. V.; Kapyshev, A. G.; Venevstev, Y. N.; Zhdanov, G. S. *Izvest. Akd. Nauk SSSR, Ser. Fiz.* **1962**, *26*, 354.
(5) Smolenskii, G. A.; Isupov, V. A.; Agranovskaya, A. I.; Krainik, N. N. *Sov. Phys.-Solid State* **1961**, *2*, 2651.
(6) Vakhrushev, S. V.; Kvyatkovsky, B. E.; Malysheva, R. S.; Okuneva, N. M.; Plachenova, E. L.; Syrnikov, P. P. *Kristallografiya* **1989**, *34*, 154 [*Sov. Phys. Crystallogr.* **1989**, *34*, 89].
(7) Zvirgzds, J. A.; Kapostins, P. P.; Zvirgzde, J. V.; Kruzina, T. V. *Ferroelectrics* **1982**, *40*, 75.
(8) Park, S.-E.; Chung, S.-J.; Kim, I.-T.; Hong, K. S. *J. Am. Ceram. Soc.* **1994**, *77*, 2641.
(9) Pronin, I. P.; Syrnikov, P. P.; Isupov, V. A.; Egorov, V. M.; Zaitseva, N. V. *Ferroelectrics* **1980**, *25*, 395.

10.1021/cm9806533 CCC: $18.00
Published on Web 12/30/1998

lish the presence of either the 111 or 100 reflections, this conclusion must be considered tentative.

Unlike its structure, the dielectric behavior of BNT is fairly well-characterized. The dielectric constant of BNT rises from a value of approximately 500 at room temperature to a maximum in excess of 2000 in the tetragonal phase region, near 300 °C. It has long been accepted that the rhombohedral phase of BNT is ferroelectric while the cubic phase is paraelectric. Considerable debate has surrounded the dielectric behavior of the tetragonal phase, but recent studies give good reason to believe that the tetragonal phase, like the cubic phase, is paraelectric.[11,12]

The high dielectric constant of BNT makes it potentially useful in piezoelectric devices (i.e., ultrasonic generators, actuators).[13] The technological applications of BNT provide a strong motivation to search for isostructural analogues. Since the dielectric behavior of BNT can probably be traced back to the presence Bi^{3+}, and perhaps to a lesser extent Ti^{4+}, a logical approach is to replace Na^+ with alternative cations. In practice this approach is complicated by the lack of suitable monovalent cations which can be incorporated onto the A-site of the perovskite structure. The similarity of sodium and silver in terms of their ionic radii[14] (r_{Ag} = 1.42, r_{Na} = 1.32 Å) and A-site coordination geometry suggests that Ag^+ would be a reasonable replacement for Na^+. However, the poor thermal stability of Ag_2O prevents synthesis via a conventional solid-state reaction method.[15] Thus, until recently, there were only two perovskite materials known to contain Ag^+ on the A-site, $AgNbO_3$ and $AgTaO_3$.[16] However, using high pressure−high temperature synthesis techniques, we recently were able to prepare two new perovskites, $(Ca_{1/2}Nd_{1/4}Ag_{1/4})TiO_3$ and $NdAgTi_2O_6$, both of which contain Ag^+ on the A-site.[17] This discovery suggested that such a synthetic approach might allow us to successfully synthesize $(Bi_{1/2}Ag_{1/2})TiO_3$. This approach has proved successful, and we report herein the synthesis, structural analysis, and dielectric properties of $(Bi_{1/2}Ag_{1/2})TiO_3$.

Experimental Section

Synthesis. Polycrystalline specimens of $Bi_{1/2}Ag_{1/2}TiO_3$ were synthesized in the multianvil 2000-ton uniaxial split sphere high-pressure apparatus (USSA-2000) at Stony Brook. A stoichiometric mixture of reagent grade Bi_2O_3, Ag_2O, and TiO_2 was thoroughly ground, tightly packed in a powdered form, and then sealed in Au capsules with an inside diameter of 3.2 mm and a wall thickness of 0.1 mm. Polycrystalline samples were obtained from high-pressure treatment at 14−14.5 GPa and 1000 °C for 3 h, followed by temperature quenching and slow decompression. After recovery, the metal ratio was estimated, from electron probe microanalysis (EPMA) using BIGE ($Bi_{12}GeO_{20}$), Ag_2S, and ILMN ($FeTiO_3$) as the references for Bi, Ag, and Ti, respectively, to be $Bi_{0.99(1)}Ag_{1.00(1)}Ti_{1.86(1)}O_6$. The details of the cell assembly along with the temperature and the pressure calibration have been reported elsewhere.[18,19]

Synchrotron X-ray Diffraction. Synchrotron X-ray powder diffraction data were collected on the X7A beamline at the National Synchrotron Light Source (NSLS), located at Brookhaven National Laboratory (BNL). Samples were contained in 0.2 mm capillaries which were freely rotated at 1−2 Hz during data collection to avoid potential problems with preferred orientation or texture. The empirical absorption correction to the overall Debye−Waller factor ($\Delta B = 0.53$ Å^2) was estimated from the measured density of the filled capillary, using the formula derived by Hewat.[20] Monochromatic radiation was obtained using a channel-cut Ge(111) monochromator and calibrated using a CeO_2 standard ($a = 5.4113(1)$ Å). The data were collected in a step scan over the approximate angular range $10° < 2\theta < 60°$ in increments of 0.25° using a linear position sensitive detector (PSD).[21−23] Low-temperature X-ray diffraction spectra were collected using a two-stage Air Products Displex unit for temperature control. Upon cooling, data sets were collected at 300, 200, 100, and 15 K and, upon warming, at 50 and 100 K. High-temperature X-ray diffraction spectra were collected using a ceramic furnace for heating; data sets were collected at 298, 373, 473, 573, 673, and 773 K and during cooling at 448, 423, 398, 373, and 298 K. The structure of $(Bi_{1/2}Ag_{1/2})TiO_3$ was refined using the Rietveld method[24] as implemented in the generalized structure analysis system (GSAS).[25]

Dielectric Measurements. A plane capacitor dielectric contact measurement was made in the temperature range 273−778 K using a hot plate at a frequency of 100 kHz. Electrical contact to the cylindrical sample, 3.0 mm in diameter by 1.0 mm high, was made using copper plates and silver paste. The measurements were carried out using a Hewlett-Packard impedance analyzer, model 4192A. Due to limitations related to sample geometry, no edge correction was included and the true dielectric constant may differ from the measured values by as much as 10−20%.[26]

Electron Diffraction. Samples were dispersed in either water or ethanol and a drop was allowed to evaporate on a holey carbon support film on a copper grid. Imaging and selected-area electron diffraction (SAED) utilized a JEOL 200CX transmission electron microscope operated at 200 keV. Energy-dispersive X-ray analysis (EDX) was used for initial identification of phases.

Results

Room-Temperature Structure Analysis. The peaks in the room-temperature diffraction pattern can be indexed on an orthorhombic perovskite unit cell, with approximate dimensions $\sqrt{2}a_p \times \sqrt{2}a_p \times 2a_p$ (a_p = the simple cubic perovskite cell parameter ~ 3.9 Å). The orthorhombic cell dimensions can be inferred from the obvious splitting of peaks such as the 044 and 404 reflections ($2\theta = 33.6°$). The extinction conditions for

(10) Isupov, V. A.; Kruzia, T. V. *Izv. Akad. Nauk USSR, Seriya fiz.* **1983**, *47*, 616.
(11) Park, S.-E.; Chung, S.-J.; Kim, I.-T. *J. Am. Ceram. Soc.* **1996**, *79*, 1290.
(12) East, J.; Sinclair, D. C. *J. Mater. Sci. Lett.* **1997**, *16*, 422.
(13) Takenaka, T.; Sakata, K.; Toda, K. *Jpn. J. Appl. Phys.* **1989**, *28 [Supp. 28−2]*, 59.
(14) Shannon, R. D. *Acta Crystallogr*. **1976**, *A32*, 751.
(15) Lide, D. R. (Editor) *CRC Handbook of Chemistry and Physics*, 77th ed.; CRC Press: Boca Raton, 1996−1997.
(16) Francombe, M. H.; Lewis, B. *Acta Crystallogr.* **1958**, *11*, 175.
(17) Park, J.-H.; Woodward, P. M.; Parise, J. B. *Chem. Mater.* **1998**, *10*, 3092.
(18) Park, J.-H.; Parise, J. B. *Mater. Res. Bull.* **1997**, *32*, 1617.
(19) Liebermann, R. C.; Wang, Y. *High-Pressure Research: Application to Earth and Planery Sciences*; Terrapub: Tokyo, 1992.
(20) Hewat, A. W. *Acta Crystallogr.* **1979**, *A35*, 248.
(21) Cox, D. E.; Toby, B. H.; Eddy, M. M. *Aust. J. Phys.* **1988**, *41*, 117.
(22) Cox, D. E. *Synchrotron Radiation Crystallography*; Academic Press: London, 1992.
(23) Smith, G. C. *Synch. Rad. News* **1991**, *4*, 24.
(24) Rietveld, H. M. *J. Appl. Crystallogr.* **1969**, *2*, 65.
(25) Larson, A. C.; von Dreele, R. B. General Structure Analysis System; Los Alamos National Laboratory: Los Alamos, NM, 1994.
(26) The experimental dielectric constant reported here is calculated by the equation $\kappa = CA/\epsilon_0 t$, where κ is the dielectric constant, C is the measured capacitance, ϵ_0 is the capacivity of a vacuum, t is the thickness of the sample, and A is the contact area. The actual dielectric constant may be larger than that reported here due to the effects of porosity (the relative density of the sample is 0.92) and the coexistence of 1.33 wt % srilankite. Kingery, W. D.; Bowen, H. K.; Uhlmann, D. R. *Intorduction to Ceramics;* Wiley: New York 1986.

Table 1. Crystallographic Data for $Bi_{1/2}Ag_{1/2}TiO_3$ at Various Temperatures

	15K	300K	573K	673K
wavelength (Å)	0.698413	0.650653	0.800139	0.800139
2θ range (deg)	9.5−60	3−60	10−50	10−50
space group	*Ibam*	*Ibam*	*I*4/*mcm*	$Pm\bar{3}m$
cell parameters (Å)	$a = 5.47309(8)$	$a = 5.48970(4)$	$a = 5.51664(8)$	$a = 3.90607(8)$
	$b = 5.5098(1)$	$b = 5.51954(5)$	$c = 7.8134(2)$	
	$c = 7.7563(1)$	$c = 7.77585(7)$		
no. of variables	16	15	7	4
no. of reflections	195	260	72	17
R_{wp}	0.0544	0.0248	0.0719	0.1442
R_p	0.0439	0.0175	0.0564	0.1003
$R(F^2)$	0.1163	0.1184	0.0927	0.1982
reduced χ^2	3.862	2.603	3.310	8.064

Table 2. Fractional Coordinates and Equivalent Isotropic Displacement Coefficients (Å²) at 15, 300, 573, and 673K

Ibam at 300 and 15 K

	x	*y*	*z*	occupancy	U_{iso}(300K)	U_{iso}(15K)
Bi[a]	0.5	0	0.25	0.5		
Ag[a]	0.5	0	0.25	0.5		
Ti	0	0	0	1.0	0.0094(2)	0.0024(3)
O(1)	0	0	0.25	1.0	0.038(3)	0.049(5)
O(2)						
300K	0.210(1)	0.712(1)	0	1.0	0.014(2)	
15K	0.210(2)	0.716(2)	0	1.0		0.020(3)

	U_{11}	U_{22}	U_{33}	U_{12}	U_{13}	U_{23}
300K	0.0214(5)	0.0640(6)	0.0251(6)	0.0	0.0	0.0
15K	0.0067(5)	0.0552(9)	0.0160(7)	0.0	0.0	0.0

	x	*y*	*z*	occupancy	U_{iso}
			*I*4/*mcm* at 573 K		
Bi[b]	0.5	0	0.25	0.544(9)	0.0400(3)
Ag[b]	0.5	0	0.25	0.456(9)	0.0400(3)
Ti	0	0	0	1.0	0.0043(6)
O(1)[c]	0	0	0.25	1.0	0.007(1)
O(2)[c]	0.217(1)	0.717(1)	0	1.0	0.007(1)
			$Pm\bar{3}m$ at 673 K		
Bi[b]	0.5	0.5	0.5	0.5	0.0437(8)
Ag[b]	0.5	0.5	0.5	0.5	0.0437(8)
Ti	0	0	0	1.0	0.012(1)
O(1)	0.5	0	0.0	1.0	0.036(3)

[a] Anisotropic displacement parameters of Bi/Ag are restrained as U_{ij}(Bi) = U_{ij}(Ag). [b] Isotropic displacement parameters of Bi and Ag were constrained to be the same. [c] Isotropic displacement parameters of both oxygen ions were constrained to be same.

$(Bi_{1/2}Ag_{1/2})TiO_3$ are consistent with the space groups *Ibam* (No. 72) and *Iba*2 (No. 45).[27] Refinements were carried out in both space groups, but the *Iba*2 refinements provided neither a better fit to the observed pattern nor more reasonable bond distances. Therefore, the centrosymmetric space group *Ibam* (No. 72) was selected as the space group.

In the first stage of the refinement, it was assumed that the A-site was occupied by equal concentrations of Bi^{3+} and Ag^+, based on the EPMA results. Later refinements including occupancy factors of all the metal sites showed no appreciable deviation from the ideal $(Bi_{1/2}Ag_{1/2})TiO_3$ stoichiometry. This is in contradiction with EMPA results, which indicated a deficiency of titanium. However, since the accuracy of the diffraction method is typically higher than that of EPMA, the available evidence suggests that the true stoichiometry is relatively close to the ideal stoichiometry. The apparent error in the titanium content, as determined by EPMA, may be related to the choice of standards employed in the EPMA calibration.

Table 3. Selected Interatomic Distances (Å) and Angles (deg)

	15 K	300 K	574 K
Ti−O(1) × 2	1.93907(3)	1.94396(2)	1.95336(4)
Ti−O(2) × 2	1.941(12)	1.964(8)	1.967(1)
Ti−O(2) × 2	1.984(12)	1.976(8)	1.967(1)
O(1)−Ti−O(1)	180.0	180.0	180.0
O(1)−Ti−O(1) × 4	90.0	90.0	90.0
O(1)−Ti−O(2) × 4	90.0	90.0	90.0
O(2)−Ti−O(2) × 2	90.57(10)	90.36(7)	90.0
O(2)−Ti−O(2) × 2	89.43(10)	89.64(7)	90.0
O(2)−Ti−O(2) × 2	180.0	180.0	180.0
Ag/Bi−O(2) × 4	2.551(7)	2.544(4)	2.585(7)
Ag/Bi−O(2) × 4	2.952(8)	2.974(4)	2.948(8)
Ag/Bi−O(1) × 2	2.73654(4)	2.74485(2)	2.75832(4)
Ag/Bi−O(1) × 2	2.75487(5)	2.75977(3)	2.75832(4)
Ti−O(1)−Ti	180.0	180.0	180.0
Ti−O(2)−Ti	163.3(6)	162.4(3)	165.0(6)
average ⟨Ti−O⟩	1.95469	1.96132	1.96265
Δ[a]	0.1126	0.04541	0.01121
σ^2 [b]	0.1181	0.04713	0
tilting angle	8.46	8.94	7.50

[a] The bond-length distortion, Δ,[29] is defined as $1/n \sum\{(r_i - \langle r\rangle)/\langle r\rangle\}^2 \times 10^3$. [b] The bond angle variance, σ^2,[30] is defined as $\sum[(\theta_i - 90)^2/(n-1)]$.

Isotropic displacement parameters were initially used for all sites, but the displacement parameter associated with the Bi/Ag site was found to be abnormally large. The subsequent use of an anisotropic displacement parameter for the A-site led to a significant improvement in the fit. Refinements also show quantitatively the presence of 1.33 wt % of srilankite, a high-pressure polymorph of TiO_2.[28] This phase is qualitatively observed by EDX as well. The crystallographic data and the refinement parameters are summarized in Tables 1 and 2, and select bond distances and angles are given in Table 3. The observed, calculated, and difference patterns from the Rietveld refinement are shown in Figure 1, and a representation of the structure is given in Figure 2.

The diffraction pattern shows several very weak peaks in the low-angle region. These peaks cannot be indexed with either the aforementioned orthorhombic unit cell or the srilankite unit cell. They can, however, be indexed reasonably well using a supercell with approximate dimensions $3\sqrt{2}a_p \times 2\sqrt{2}a_p \times 4a_p$. Our initial interpretation of this observation was that these peaks arose as a consequence of either weak Bi^{3+}/Ag^+ ordering or cooperative displacements of the Bi^{3+} ions. To investigate the possibility of a supercell further, selected area electron diffraction (SAED) patterns were taken. Due to strong preferred orientation and high absorption problems, only SAED patterns as shown in

(27) *International Tables for Crystallography*; Hahn, T., Ed.; IUCr: Dordrecht, 1987; Vol. A.

(28) Willgallis, A.; Hantl, H. *Z. Kristallogr.* **1983**, *164*, 59.

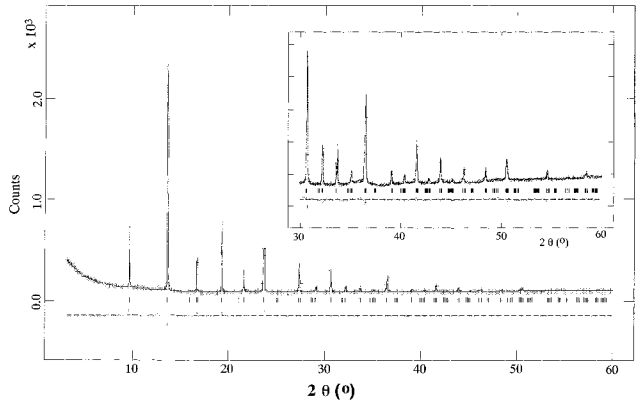

Figure 1. The observed, calculated, and difference patterns from the room-temperature Rietveld refinement of $(Bi_{1/2}Ag_{1/2})TiO_3$. The tick marks indicate the positions of reflections from $(Bi_{1/2}Ag_{1/2})TiO_3$. The difference curve is shown at the bottom on the same scale. The high angle area ($30° < 2\theta < 60°$) is magnified.

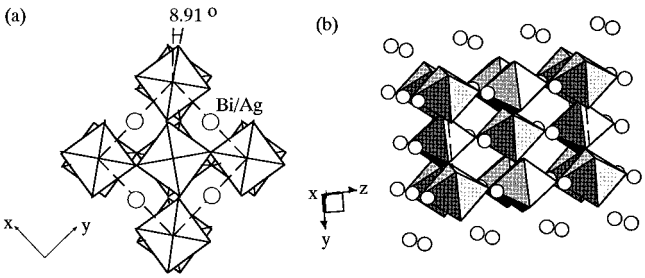

Figure 2. Projection of the structure (a) on the *xy* plane showing the 8.91(2)° octahedral tilting angle about the *c* axis. (b) TiO_6 octahedral linkages of $(Bi_{1/2}Ag_{1/2})TiO_3$. Open circles represent disordered Bi/Ag sites. The large thermal parameter of the Bi^{3+}/Ag^{+} ions along ⟨010⟩ is significant.

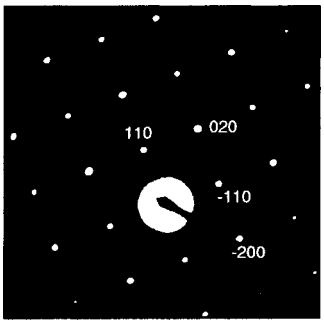

Figure 3. The SAED pattern of $(Bi_{1/2}Ag_{1/2})TiO_3$, which coincides with the (*hk*0) plane of the orthorhombic unit cell. The SAED pattern was indexed on the basis of the unit cell parameters determined from powder diffraction at room temperature
($a = 5.48970$ Å, $b = 5.51954$ Å).

Figure 3 were obtained. Surprisingly, the SAED results give no indication of a supercell, but rather confirm the $\sqrt{2}a_p \times \sqrt{2}a_p \times 2a_p$ lattice obtained in the powder diffraction study.

Temperature-Dependent X-ray Diffraction Studies. The variable temperature diffraction studies revealed no phase transitions below room temperature (300−15 K). Rietveld refinements confirm *Ibam* symmetry at 15 K. In contrast, diffraction studies conducted between room temperature and 773 K reveal two high-temperature phase transitions. Though the existence of broad peaks makes it ambiguous to clarify the symmetry at 473 K, the peak splitting and extinction

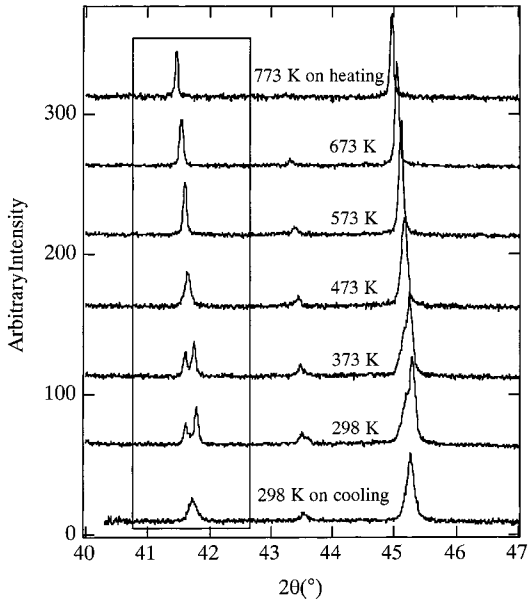

Figure 4. The powder X-ray diffraction patterns ($40° < 2\theta < 47°$) of $(Bi_{1/2}Ag_{1/2})TiO_3$ at elevated temperatures. The reduction and disappearance in the peak splitting of 404 and 044 reflections around 42° (shown in the box) illustrates the evolution of the structure upon heating from orthorhombic (*Ibam*), to tetragonal ($I4/mcm$), and finally to cubic ($Pm\bar{3}m$). At the bottom, the X-ray diffraction pattern taken after cooling back to 298 K shows the irreversible phase transition induced by heating.

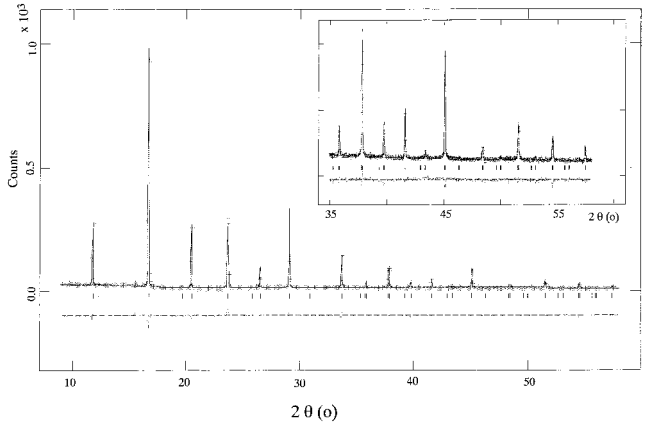

Figure 5. The observed, calculated, and difference patterns from the Rietveld refinement of $(Bi_{1/2}Ag_{1/2})TiO_3$ at 573 K, in the tetragonal phase. The tick marks indicate the positions of reflections from $(Bi_{1/2}Ag_{1/2})TiO_3$. The difference curve is shown on the bottom on the same scale. The high angle area ($35° < 2\theta < 60°$) is magnified.

conditions at 573 K are clearly consistent with a body-centered tetragonal cell, and at 673 K, the structure has evolved to a simple cubic perovskite. Note in Figure 4 that the splitting of the 404 and 044 peaks, indicative of an orthorhombic unit cell, disappears above the orthorhombic−tetragonal phase transition. The tetragonal structure has $I4/mcm$ symmetry, as expected for a member of the $a^0a^0c^-$ tilt system, with unit cell dimensions $a = b = 5.51664(8)$ Å and $c = 7.8134(2)$ Å. The observed, calculated, and difference curves at 573 K are shown in Figure 5. The cubic structure has $Pm\bar{3}m$ symmetry, with a cell edge of 3.90607(8) Å at 673 K. The refinement results at 15, 300, 573, and 673 K are summarized in Tables 1−3. In Figure 6, lattice parameters as a function of temperature are shown. At 15,

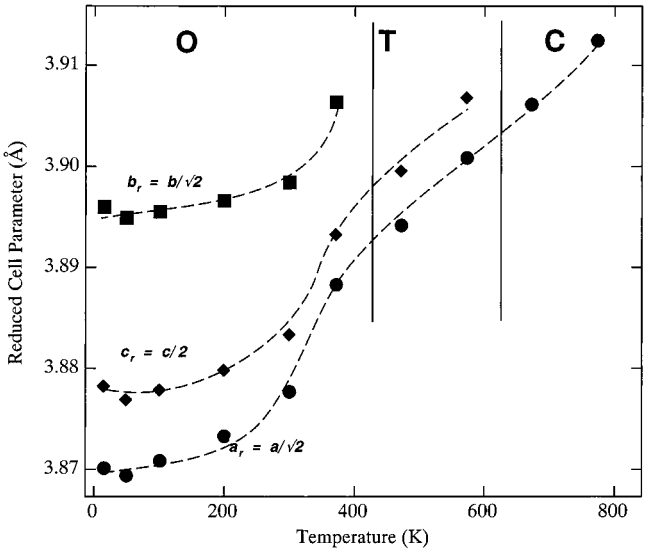

Figure 6. The lattice parameter (Å) evolution as a function of temperature (K). The reduced cell parameters, a_r, b_r, and c_r, are related to the orthorhombic cell parameters by the relationships $a/\sqrt{2}$, $b/\sqrt{2}$, and $c/2$ and to the tetragonal cell parameters by $a/\sqrt{2}$ and $c/2$.

300, and 573 K, the distortions of the TiO_6 octahedra were quantified in terms of the bond length distortion, Δ,[29] and the bond angle variance, σ^2.[30] The results of these calculations are given in Table 3. These calculations show that the octahedral distortion decreases as the temperature increases.

An unusual aspect of the phase transition behavior of this compound is that the orthorhombic phase is not recovered upon cooling back to room temperature, as shown in Figure 4. No splitting of the 404 and 044 reflections, indicative of an orthorhombic distortion of the unit cell, can be detected in the patterns collected upon cooling. The explanation for this curious behavior is thought to be related to a change in the composition under high temperature/ambient pressure conditions and will be discussed in more detail below.

Dielectric Properties. The capacitance, as a function of temperature, is shown in Figure 7. At room temperature the dielectric constant is 354. Upon heating, the capacitance gradually increases, with a local maximum corresponding to a dielectric constant of 834 near 580 K. It should be noted that the maximum occurs in the temperature range where the tetragonal phase is stabilized. At higher temperatures, the capacitance shows a shallow decrease and then a broad peak around 738 K, corresponding to a dielectric constant of 1308. We believe that this feature is related to the decomposition of $(Bi_{1/2}Ag_{1/2})TiO_3$. As the temperature returns to ambient conditions, the capacitance behaves quite differently, showing a first-order transition at 608 K, followed by a steady decrease. To explore the possibility of an irreversible phase transformation, as suggested by the diffraction results, we repeated the measurement on the same sample. The capacitance in this second measurement showed a near linear dependence on the temperature (338.6 K < T < 621.3 K) with similar magnitude. An Arrhenius plot of the conductivity vs

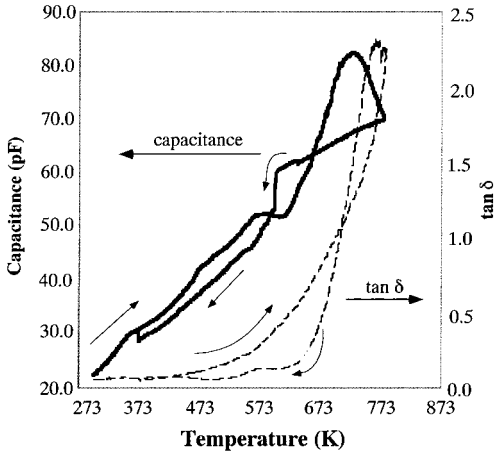

Figure 7. Measurement of the capacitance as a function of temperature in the first run. The bold and dashed lines represent the capacitance and tan δ, respectively.

temperature gives an activation energy of 0.0808(4) eV. To investigate partial decomposition of the sample, the silver paste was removed from the surface of the sample, using a fine grain sand paper, and X-ray powder diffraction and EPMA were performed.

The diffraction pattern of the recovered material indicated the presence of a perovskite phase, as expected, indicating that no major decomposition had occurred; this is consistent with the synchrotron XRD patterns collected upon cooling. However, a previously unobserved minor peak (d = 3.6348 Å) was evident. The EPMA generally confirmed the original composition, but some variation in the silver content across the sample was observed. We suspect that this unusual behavior is caused by the migration of a small amount of silver. Studies of the dielectric constant as a function of frequency are planned for the near future.

Discussion

Structure. The structure of $(Bi_{1/2}Ag_{1/2})TiO_3$ at high temperature is a simple cubic perovskite. The tetragonal structure of $(Bi_{1/2}Ag_{1/2})TiO_3$ is distorted from cubic by antiphase rotations of the TiO_6 octahedra about the z axis. It is isostructural with the low temperature form of $SrTiO_3$.[31] Using Glazer notation, which is a concise and useful way to describe octahedral tilting distortions in perovskites, the $I4/mcm$ structure corresponds to the $a^0a^0c^-$ tilt system.[32−34] Therefore, at least in terms of the average structure, the cubic and tetragonal modifications of $(Bi_{1/2}Ag_{1/2})TiO_3$ can be well understood. On the other hand, the orthorhombic *Ibam* modification does not correspond to any previously documented distortion of the cubic perovskite structure. To understand this structure we first note that *Ibam* is an isomorphic subgroup of $I4/mcm$. Comparing the coordinates of the various sites in the two space groups reveals that the Ag/Bi, Ti, and O(1) atoms have identical coordinates in $I4/mcm$ and *Ibam*. The O(2) atom is not constrained by symmetry to have the same coordinates

(29) Sasaki, S.; Prewitt, C. T.; Liebermann, R. C. *Am. Mineral.* **1983**, *68*, 1189.
(30) Robinson, K.; Gibbs, G. V.; Ribbe, P. H. *Science* **1971**, *172*, 567.
(31) Unoki, J.; Sakudo, T. *J. Phys. Soc. Jpn.* **1967**, *23*, 546.
(32) Glazer, A. M. *Acta Crystallogr.* **1972**, *B28*, 3385.
(33) Burns, G.; Glazer, A. M. *Space Groups for Solid State Scientists*, 2nd ed.; Academic Press: Boston, 1990; Appendix A9−6.
(34) Woodward, P. M. *Acta Crystallogr.* **1997**, *B53*, 32.

Table 4. Cation Bond Valences with Bi on the Ideal Site (4a) and in a Split Position (8g)

	Bi in (4a)	Bi in (8g)
Ag	1.02	1.02
Bi	2.21	2.31
Ti	4.04	4.05

in the two space groups, but in practice, the refined coordinates differ by very little, as shown in Table 2.

Thus $a^0a^0c^-$ octahedral tilting appears to be the only distortion mechanism present in both tetragonal and orthorhombic modifications. What then is responsible for the orthorhombic distortion? The answer to this question lies in the lattice and displacement parameters associated with the *Ibam* structure. The anisotropic displacement parameters of the Ag/Bi site are much larger parallel to the *b*-axis than they are in the other directions. The large anisotropy observed at 300 K and the fact that it persists down to 15 K indicate static, randomly oriented displacements of either one or both of the A-site cations off of the ideal site. To make room for this displacement, an expansion of the *b*-axis occurs, lowering the symmetry from tetragonal to orthorhombic.

Several factors support a conclusion that bismuth is responsible for the A-site displacements. Foremost, Bi^{3+} has two 6s electrons, which are capable of mixing with a 6p orbital to form a stereoactive lone electron pair. This tendency is enhanced by Ag^+ being larger ($r = 1.42$ Å) than Bi^{3+} ($r = 1.31$ Å), which in the absence of strong local relaxation effects will put the Bi−O bonds in tension. This picture is consistent with the low bond valence sum calculated for Bi^{3+} on the ideal site (Table 4). Such a coordination environment destabilizes an isotropic Bi−O bonding arrangement, with respect to the directional bonding which accompanies the development of a stereoactive lone electron pair. In an attempt to quantify the displacement of the Bi^{3+} ion, refinements using the 300 K data set were carried out with Bi^{3+} on a split position (Ag^+ was kept on the ideal site). When Bi^{3+} was placed on the 8g site (1/2, *y*, 1/4) with occupancy 0.25 and isotropic displacement parameters for all ions, the refined value of *y* was −0.0445(3). This corresponds to a displacement of 0.246(2) Å and results in a 4.5% improvement of the Bi^{3+} bond valence sum. Despite this displacement from the ideal site, the bond valence of the bismuth ion is still lower than its ideal value of 3.0, and the displacement is considerably smaller than the 0.634 Å shift observed in $BiFeO_3$.[35] Statistically the split position and anisotropic displacement parameter models give equivalent fits to the experimental data.

It is informative to compare the structures of $(Bi_{1/2}Ag_{1/2})TiO_3$, $(Bi_{1/2}Na_{1/2})TiO_3$, and $NdAgTi_2O_6$.[17] Among these compounds there are three mechanisms responsible for distortion from the cubic perovskite structure: A-site cation ordering, octahedral tilting, and cation displacements. Considering first cation ordering, diffraction studies show that in $NdAgTi_2O_6$ there is a partial segregation (ordering) of the Nd^{3+}/Ag^+ cations into alternating layers, perpendicular to the *z* axis. This layered A-site cation ordering, which is driven by the charge and size difference between Nd^{3+} and Ag^+, leads to a tetragonal unit cell. Though there have been some reports of long-range cation ordering in $(Bi_{1/2}Na_{1/2})TiO_3$, the supporting evidence for such claims is unconvincing. Furthermore, on the basis of the ionic radii of the respective A-site cations ($Nd^{3+} = 1.249$ Å, $Bi^{3+} = 1.31$ Å, $Na^+ = 1.32$ Å, $Ag^+ = 1.42$ Å), there would appear to be a smaller driving force for ordering in $(Bi_{1/2}Na_{1/2})TiO_3$ than in the other two compounds. Long-range cation ordering is also absent in $(Bi_{1/2}Ag_{1/2})TiO_3$, but the cooperative Bi^{3+} shifts that result in a ferroelastic orthorhombic distortion suggest the possibility of short-range Ag^+/Bi^{3+} order.

Turning next to the question of octahedral tilting, both $NdAgTi_2O_6$ and $(Bi_{1/2}Ag_{1/2})TiO_3$ show antiphase rotations of the octahedra about the *z* axis (tilt system $a^0a^0c^-$), as shown in Figure 2. The octahedral tilting angles are estimated from the fractional coordinates to be 7.97(1)° and 8.91(1)°, respectively. In contrast, the TiO_6 octahedra in $(Bi_{1/2}Na_{1/2})TiO_3$ show antiphase rotations about the body diagonal, ⟨111⟩ (tilt system $a^-a^-a^-$). In the absence of other distortion mechanisms, $a^0a^0c^-$ tilting leads to a tetragonal unit cell, while $a^-a^-a^-$ tilting leads to a rhombohedral unit cell.

The third distortion mechanism, cation displacements, is present in both $(Bi_{1/2}Na_{1/2})TiO_3$ and $(Bi_{1/2}Ag_{1/2})TiO_3$. The displacements of the A-site cations from the center of their coordination polyhedra in these compounds are presumably driven by the need to accommodate a stereoactive lone electron pair on Bi^{3+}. This conclusion is reinforced by the observation that such displacements are absent in $NdAgTi_2O_6$. In $(Bi_{1/2}Na_{1/2})TiO_3$, these displacements are cooperative and directed along the ⟨111⟩ direction of the cubic perovskite unit cell. Cation displacements along ⟨111⟩ are known to lead to a rhombohedral distortion of the unit cell and are compatible with the rhombohedral distortion caused by the $a^-a^-a^-$ octahedral tilting distortion. In $(Bi_{1/2}Ag_{1/2})TiO_3$, cooperative A-site cation displacements are not allowed within the observed *Ibam* space group. However, as discussed above, the displacement parameters, orthorhombic distortion, and dielectric behavior of this compound give compelling evidence for local shifts of the Bi^{3+} ions along the ⟨010⟩ direction of the orthorhombic cell. One can speculate that short-range layered Ag^+/Bi^{3+} ordering stabilizes the $a^0a^0c^-$ tilt system over the $a^-a^-a^-$ tilt system, since the former tilt system leads to a tetragonal distortion of the unit cell, just as layered cation ordering does. This in turn influences the directionality of the Bi^{3+} shifts.

Dielectric Properties. The magnitude and temperature-dependent behavior of both the dielectric constant and loss of $(Bi_{1/2}Ag_{1/2})TiO_3$ are quite similar to the dielectric properties exhibited by $(Bi_{1/2}Na_{1/2})TiO_3$. From this observation it seems likely that $(Bi_{1/2}Ag_{1/2})TiO_3$ is ferroelectric in the orthorhombic phase. However, this conclusion is not supported by the refinement results, which indicate a centrosymmetric space group. The most probable explanation for this apparent contradiction is that the local structure is polar, but the ion displacements are not cooperative on a long-range scale, so the average structure appears centrosymmetric. The lack of long-range order in the ion displacements is a common structural feature found in relaxor ferroelectrics, implying that $(Bi_{1/2}Ag_{1/2})TiO_3$ is a new member of this important class of materials. To definitively char-

(35) Thomas, N. W.; Beitollahi, A. *Acta Crystallogr.* **1994**, *B50*, 549.

acterize the dielectric behavior of $(Bi_{1/2}Ag_{1/2})TiO_3$, we are currently examining the frequency dependent dielectric behavior and looking for hysteresis loops.

Acknowledgment. J.-H.P. and J.B.P. appreciate the financial support of the NSF (DMR-9713375/EAR-8920239). The high-pressure experiments in this study were performed at the Stony Brook High Pressure Laboratory, which is jointly supported by the State University of New York at Stony Brook and the NSF Science and Technology Center for High Pressure Research (Grant EAR 89-20239). This work was also partially supported by the Division of Materials Sciences, U.S. Department of Energy, under contract No. DE-AC02-98CH10886. The NSLS is supported by the U.S. Department of Energy, Division of Materials Sciences and Division of Chemical Sciences.

CM9806533